

Article

Extreme Heights of 15 January 2022 Tonga Volcanic Plume and Its Initial Evolution Inferred from COSMIC-2 RO Measurements

Saginela Ravindra Babu¹ and Neng-Huei Lin^{1,2}

¹ Department of Atmospheric Sciences, National Central University, Taoyuan 32001, Taiwan.

² Center for Environmental Monitoring and Technology, National Central University, Taoyuan 32001, Taiwan.

* Correspondence: S. Ravindra Babu (baburavindra595@gmail.com) and Neng-Huei Lin (nhlin@cc.ncu.edu.tw).

Abstract: The Hunga Tonga-Hunga Ha'apai underwater volcano (20.57°S, 175.38°W) violently erupted on 15 January 2022. The volcanic plume evolution during its initial stages is delineated by using Constellation Observing System for Meteorology, Ionosphere, and Climate (COSMIC)-2 radio occultation (RO) measurements. The bending angle (BA) anomaly over the Tonga volcanic plume (within 200 km from the eruption center) at 5:17 UTC on 15 January shows a prominent peak at higher stratospheric heights. The top of the BA anomaly revealed that negative to positive change occurred at ~38 km indicating the first height where the RO line-of-sight encounters the volcanic plume. The BA anomaly further revealed an increase of ~50% at ~36 km and confirms the volcanic plume reached above ~36 km. Further, the evolution of BA perturbations within 24 hours after the initial explosion is also discussed. From collocated RO profiles with the volcanic plume, we find a clear descending of the peak altitude of the BA perturbation from ~36 km to ~30 km within 24 hours after the initial eruption. The results from the study will provide some insights into advancing our understanding of volcanic cloud dynamics and their implementation in volcanic plume modeling.

Keywords: Tonga Volcano; COSMIC-2 RO; Thermal structure; stratospheric water vapor

1. Introduction

On 15 January 2022, the underwater volcano in Hunga Tonga-Hunga Ha'apai (hereafter Tonga eruption) island (20.57°S, 175.38°W) erupted violently at 17:30 local time (4:30 UTC) and released enormous amounts of energy, ash, gases, and steam into the atmosphere (Global Volcanism Program, 2022). The eruption also triggered tsunami waves around the Pacific Ocean (Adam, 2022; Carvajal et al., 2022), atmospheric gravity waves (GWs), and Lamb waves into the atmosphere (Wright et al., 2022; Matoza et al., 2022; Proud et al., 2022). Liu et al. (2022) reported strong GWs with amplitudes greater than 30 K (twice the usual GWs) in the mesosphere associated with the Tonga volcano eruption. Several weather stations worldwide detected atmospheric pressure changes that were among the most extraordinary ever recorded. The geostationary GOES-17 and Himawari-8 satellites captured this explosive eruption and showed volcanic plume dispersion. According to preliminary reports from the Global Volcanism Program (2022), the volcanic plume was lofted as high as ~40 km into the stratosphere, a record in the modern satellite era and which was not seen in the previous eruptions that occurred in the 21st century (Tournigand et al., 2020). Some cloud portions even reached lower mesospheric altitudes (NASA Earth Observatory, 2022). These preliminary reports are further supported by a recent study by Carr et al. (2022). Based on GOES-17 and Himawari-8 stereo observations, Carr et al. (2022) reported that the main umbrella cloud of Tonga reaches about 35–40 km, while parts of the center plume reached as high as ~55 km. It is unclear why this eruption was so violent and why the volcanic substances were lofted to extreme

heights compared to the other explosions in the 21st century. It is suggested that 'the involvement of water in the Tonga eruption may have increased the explosivity of the Tonga eruption on 15 January' (NASA Earth Observatory, 2022).

Global Navigation Satellite System (GNSS) radio occultation (RO) measurements, particularly the Constellation Observing System for Meteorology, Ionosphere, and Climate (COSMIC), have been widely used for understanding the vertical thermal structure changes due to the volcanic eruptions (Wang et al., 2009; Okazaki and Heki, 2012; Biondi et al., 2017; Ravindra Babu and Liou, 2022). Wang et al. (2009) and Okazaki et al. (2012) used for the first time GNSS RO to study the effect of volcanic eruptions on atmospheric temperature by comparing RO profiles before and after the explosion. Biondi et al. (2017) extensively used COSMIC RO data to detect the volcanic cloud top altitude from the bending angle anomaly. Similarly, Ravindra Babu and Liou (2022) reported day-to-day atmospheric temperature variability in response to the Taal volcanic eruption in 2020 by using recently launched COSMIC-2 RO data. All the studies mentioned above reported the atmospheric thermal structure after the eruption, while, mainly focusing on the upper troposphere and lower stratosphere (UTLS) region. Also, it is noted that none of the previous eruptions in the 21st century had reached such heights as the Tonga eruption. The high-density measurements from the COSMIC-2 mission (Schreiner et al., 2020) provide a unique opportunity to describe the Tonga volcanic cloud and its evolution. By taking this advantage, in the present study, we attempt to demonstrate the extreme heights of Tonga eruption and its initial evolution within 24 hours by utilizing COSMIC-2 RO measurements.

2. Data and Methodology

We utilized Global Navigation Satellite System (GNSS) radio occultation (RO) dry temperature profiles acquired onboard COSMIC-2 satellites. The COSMIC-2 mission, launched on 25 June 2019, collects more than 5000 RO soundings per day over the tropics and subtropics (Ho et al., 2019). The basic advantage of the COSMIC-2 mission is that it is currently taking frequent measurements over the tropics and providing higher numbers of RO profiles in a single day compared to the previous missions due to its low inclination of $\sim 24^\circ$. The data is downloaded from the COSMIC Data Analysis and Archive Centre (CDAAC) website (<https://data.cosmic.ucar.edu/gnss-ro/cosmic2/nrt/level2/>). This data was validated and compared with independent data, including radiosondes, model forecasts, and re-analysis (Schreiner et al., 2020). The details of the temperature retrieval from the bending angle and refractivity profile obtained from the GNSS RO sounding are presented elsewhere (Kursinski et al., 1997; Kuo et al., 2004; Anthes et al., 2008; Schreiner et al., 2007). The major advantage properties of the COSMIC RO temperatures are high accuracy (less than 1 K) and precision (less than 0.05 K) (Schreiner et al., 2007), and also all-weather capability.

Apart from COSMIC-2 RO, we also used version 5.0 water vapor measurements from the Microwave Limb Sounder (MLS) instrument, operating onboard the NASA Aura satellite. The data was downloaded from the following website https://acd-disc.gesdisc.eosdis.nasa.gov/data/Aura_MLS_Level2/ML2H2O.005/. More details about version 5.0 WV data can be found in Livesey et al. (2021), respectively. The Ozone Monitoring Instrument (OMI) sulfur dioxide (SO₂) upper tropospheric and stratospheric SO₂ column (corresponding to the center of mass altitude of 18 km) data were also used. Details of the retrieval technique are documented by Li et al. (2017).

To distinguish different aerosol subtypes in the atmosphere during Tonga volcanic eruption, imageries from the Cloud-Aerosol Lidar with Orthogonal Polarization (CALIOP), aboard the Cloud-Aerosol Lidar and Infrared Pathfinder Satellite Observations (CALIPSO) satellite, were also utilized in this study (Version 4.10; Anselmo, 2006; Young and Vaughan, 2009).

3. Results and Discussion

3.1. Extreme heights of Tonga volcanic plume and its initial evolution

The Hunga Tonga-Hunga Haapai volcano (20.536°S, 175.382°W) is an underwater caldera volcano located approximately 70 km North-northwest of Tonga's capital, Nukualofa. On 15th January 2022 at approximately 4 UTC (5 pm local time) the Hunga-Tonga volcano violently erupted, producing a large volcanic cloud, shown in Figure 1. A second, smaller, eruption occurred at 8 UTC with no further large eruptions occurring thereafter. Figure 1 shows the GOES-West satellite images at each 10-minutes time step starting from 4:10 UTC to 6:00 UTC. A clear expansion of the umbrella cloud around the volcano in a near-circular pattern was evident in Figure 1 (for instance, at 04:50 UTC). The upper umbrella cloud moves westward, presumably due to advection by background stratospheric easterly winds (Sellitto et al, 2022; Millán et al, 2022).

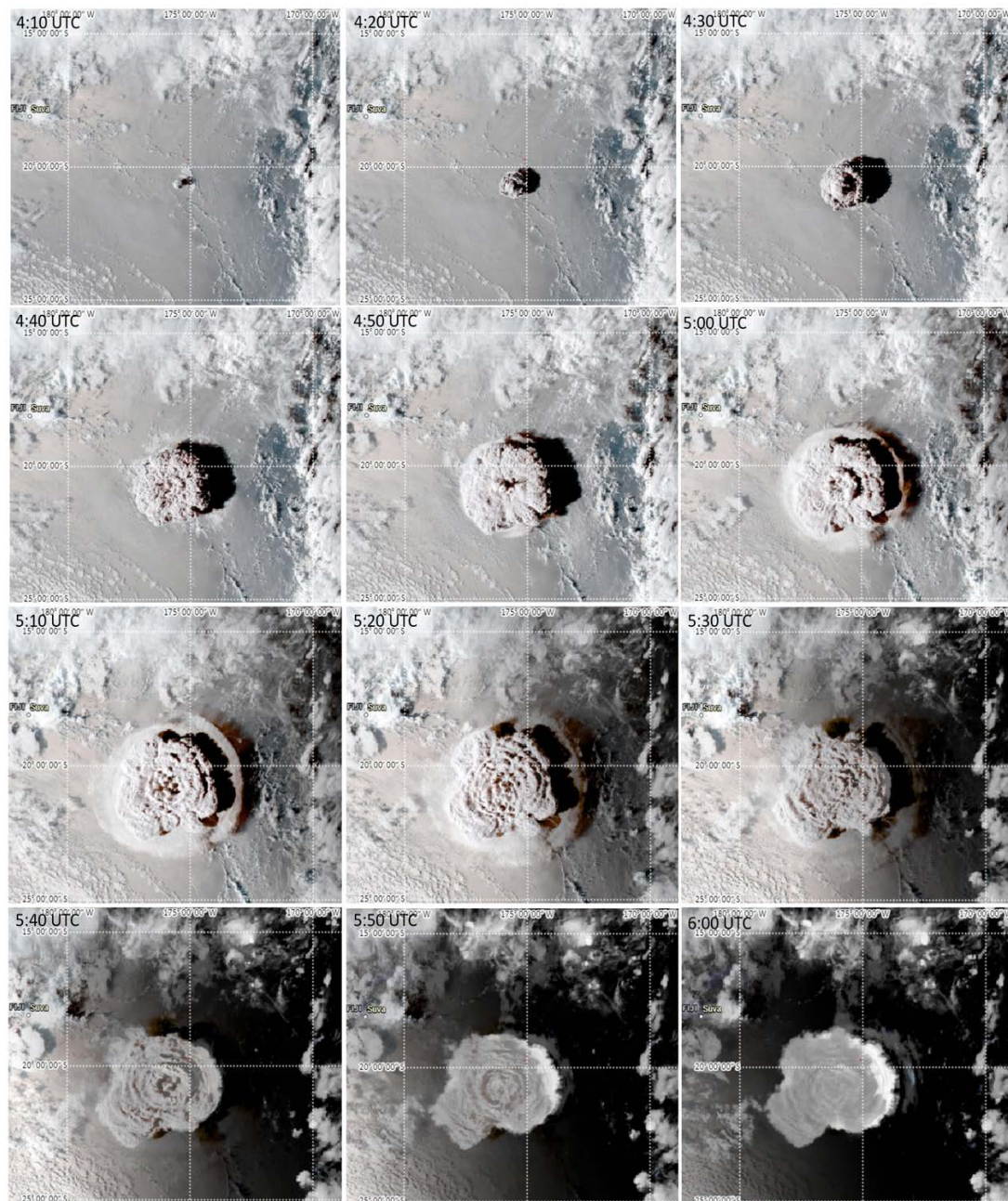


Figure 1. Geostationary Operational Environmental Satellites (GOES)-West satellite (currently, GOES-17) images observed on 15 January 2022.

To understand the dispersion and transport of volcanic plumes, a better estimation of the volcanic cloud top (VCT) altitude is crucial. Previous studies were well demonstrated the GNSS RO data for supporting the detection and monitoring of volcanic clouds as well as their effects on weather and climate. The GNSS RO bending angle anomaly method (the maximum peak in the bending angle anomaly) was used to detect the VCT altitude (Biondi et al., 2017; Cigala et al., 2019; Prata et al., 2020). We also applied a similar method to the Tonga volcanic cloud and detected the volcanic cloud heights. First, we check the availability of COSMIC-2 RO profiles during the active eruption period. Interestingly, we found two RO profiles around the Tonga volcano during its initial eruptive period. Among the available profiles, only one RO profile was found very near to the area of the eruption (hereafter eruptive profile) at 05:17 UTC (red colored dot in **Fig. 2c**), and another one at 7:11 UTC was found away from the volcano center. Quite interestingly, the time of the nearest RO profile (5:17 UTC) was around the active phase of the Tonga volcanic eruption. We looked further at the Geostationary Operational Environmental Satellites (GOES)-17 satellite images and identified the locations of these profiles which were shown as a red colored dot in **Figures 2a** and **b** (top panel). We also estimated the approximate distance of the RO profile from the center of the Tonga volcano and displayed it in **Figure 2c**, respectively. Based on **Figures 2a** and **2c**, it is very clear that the RO profile at 5:17 UTC may not be located exactly over the volcano center, instead, it looks like falling in between the center and the umbrella cloud of the volcano. It is reported that the Tonga eruption produced a large umbrella cloud with a diameter of around 500 km (Carr et al., 2022). Interestingly, the available RO profile during the active Tonga volcano eruptive period at 5:17 UTC was exactly falling within 200 km from the volcano center (**Fig. 2c**). Hence, the available RO profile at 5:17 UTC can represent the umbrella cloud of an active eruptive plume. This provides us with a more detailed analysis of the available RO profiles.

To see the bending angle anomaly (BA) for the eruptive profile at 5:17 UTC (as well as 7:11 UTC) on 15 January, we first derive a reference profile by using all the available RO profiles within the 5° latitude and longitude around the Tonga volcano. Then, we take the difference between the eruptive profile from the reference profile to find deviations near the Tonga eruption region. The obtained BA anomaly was expressed in percentage change and a prominent peak in the BA defines as the altitude of the volcanic cloud top. The obtained BA anomaly of two RO profiles is shown in **Figure 2d**, respectively. As shown in **Figure 2d**, a pronounced peak in the BA perturbation (~50% deviation from the reference profile) in the 5:17 UTC profile is observed at the altitude of about 36.1 km, suggesting the height of the volcanic plume on 15 January. The extensive peak in the BA perturbation might be due to the higher water vapor and the more likely presence of volcanic substances at the time of the active eruption. The top of the BA perturbation where the negative to positive change occurred (~38 km) indicates the first height where the RO line-of-sight encounters the volcanic plume (**Fig. 2d**). The BA analysis from the present study confirms that the height of the umbrella cloud of the Tonga eruption is ~38 km which is in line with the recent reports (NASA Earth Observatory, 2022; Proud et al., 2022; Carr et al., 2022). Further, the 7:11 UTC profile also shows a clear change in the BA between 32-35 km with a peak at ~34 km, respectively.

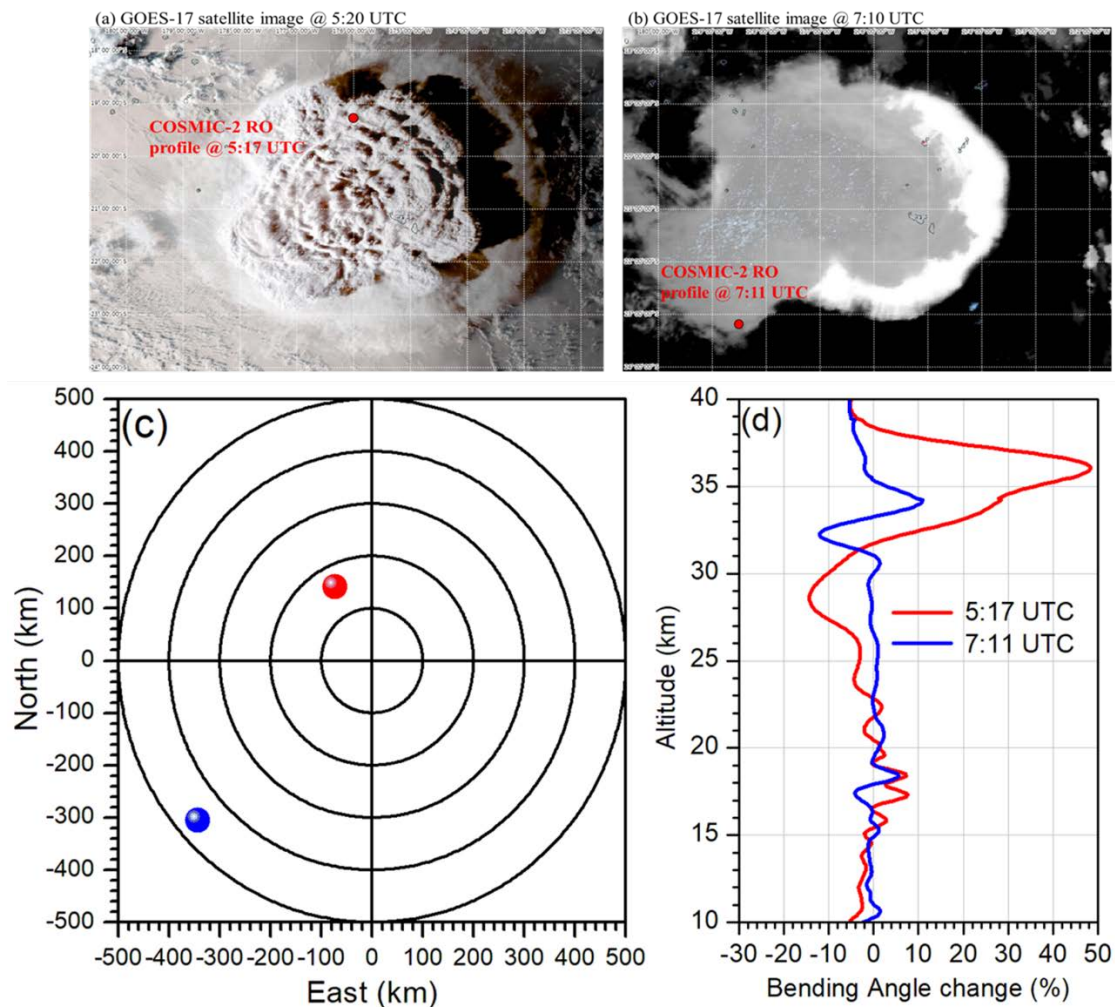


Figure 2. Top panel shows (a) GOES-17 Geo Color, Multispectral blended infrared image observed at 5:20 UTC, (b) at 7:10 UTC on 15 January 2022. The red-colored (blue) dot represents the available COSMIC-2 RO profile at 5:17 (7:11) UTC. (c) The location of above mentioned RO profile concerning Tonga volcano center. The bottom panel shows perturbations of (c) Bending Angle for above mentioned RO profile concerning the reference profile (mean of 07-13 January 2022).

After the primary eruption, we further checked the available COSMIC-2 RO profiles over the volcanic plume. Interestingly, we discovered six collocated RO profiles with the volcanic cloud after the initial eruption on 15 January. The details of the RO profiles are presented in **Table 1** (profiles 3-8), and the locations of these profiles are plotted along with OMI SO₂ data shown in **Figure 3a**, respectively. A similar method used in **Figure 2** was applied for the available RO profiles and obtained BA anomaly for each RO profile. The obtained BA anomaly profiles are plotted in **Figure 2b**, respectively. The magenta color line in **Figure 2a** shows the Cloud-Aerosol Lidar with Orthogonal Polarization (CALIOP) onboard the CALIPSO overpass at 15:20 UTC on January 15. Similarly, the vertical magenta color line shows the mean BA anomaly profile which was obtained from the average of all the available six RO profiles. A clear change in the BA anomaly can be noticed in **Figure 2b**. As observed in **Figure 2**, a significant enhancement of BA anomaly was noticed between the 30 to 35 km region with a maximum peak at ~32 km, respectively. It is noted the available RO profiles are located just near the CALIPSO overpass at 15:20 UTC. One can expect that due to CALIPSO's low signal-to-noise ratio in the stratosphere (Kar et al., 2019), it may not detect the presence of volcanic cloud above 31 km as COSMIC-2 RO detected peak BA anomaly at 32.5 km (**Fig. 3b**). However, in a recent study by Taha et al., (2022) show a clear presence of a volcanic cloud above ~32 km at 15:20 UTC on 15

January based on CALIPSO version 3.41 data. Our BA anomaly peak from **Figure 3b** is also in line with the results of Taha et al., (2022).

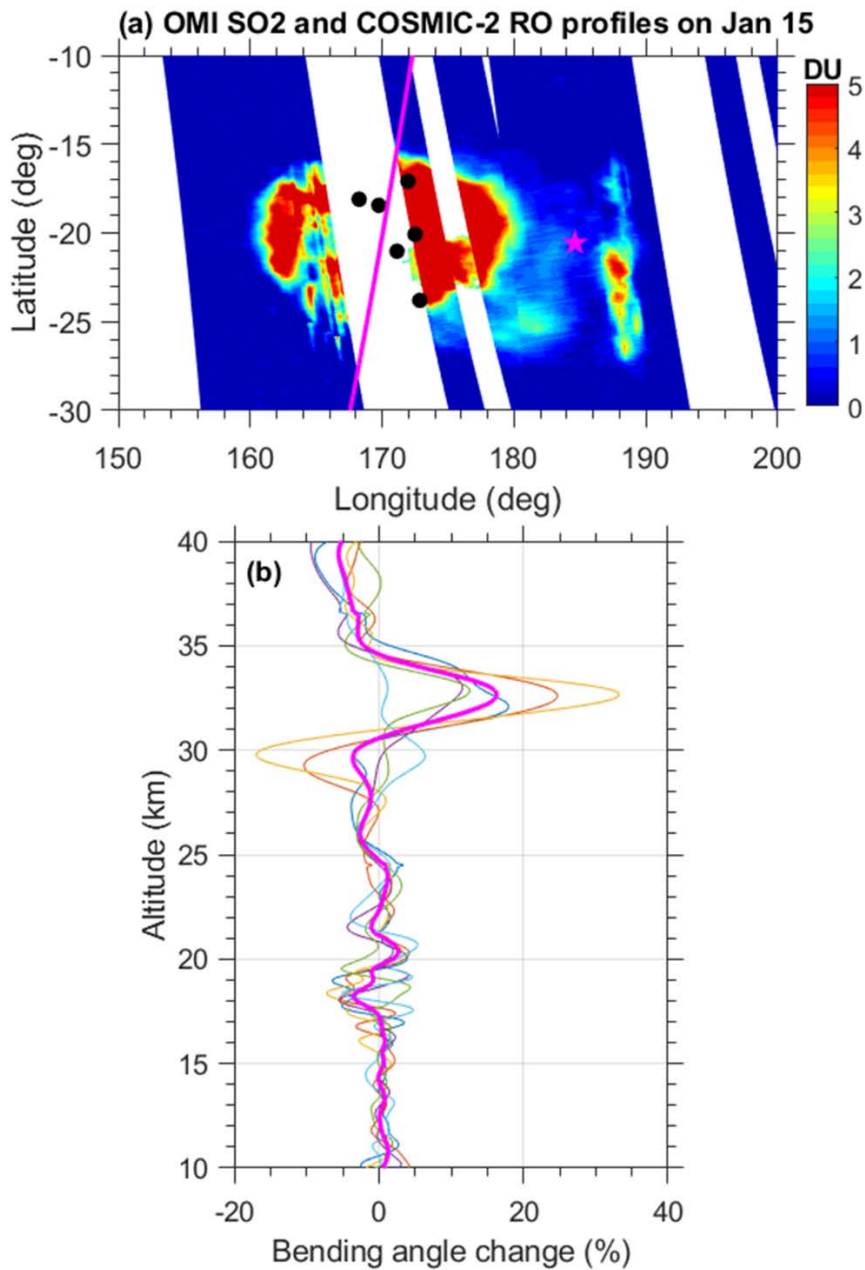


Figure 3. (a) OMI observed UTLS SO2 on 15-16 January 2022 along with the available COSMIC-2 RO profiles (black dots) on 15 January, the magenta-colored line shows the CALIPSO overpass at 15:20 UTC on 15 January, (b) bending angle (BA) percentage change for the above-mentioned RO profiles. The mean profile of BA change is shown in magenta colored-profile.

Table 1. Details of collocated COSMIC-2 radio occultation profiles with the volcanic cloud (OMI SO2) on 15 and 16 January. The highlighted file names were related to the RO profiles that are available during eruptive stage as shown in Figure 2. .

File name	Longitude	Latitude	Starting time for RO	
			Hour	Minutes
atmPrf_C2E3.2022.015.05.20.G05_0001.0001_nc	183.9595	-19.299	5	17
atmPrf_C2E3.2022.015.07.11.G08_0001.0001_nc	181.5302	-23.3197	7	11
atmPrf_C2E6.2022.015.17.47.G22_0001.0001_nc	171.1261	-21.0282	17	45

atmPrf_C2E6.2022.015.17.58.G15_0001.0001_nc	172.4965	-20.0758	17	58
atmPrf_C2E1.2022.015.18.15.R05_0001.0001_nc	172.8534	-23.7979	18	15
atmPrf_C2E4.2022.015.18.31.R05_0001.0001_nc	169.7485	-18.4442	18	31
atmPrf_C2E4.2022.015.20.13.G15_0001.0001_nc	168.2508	-18.0995	20	13
atmPrf_C2E4.2022.015.23.27.G17_0001.0001_nc	171.9524	-17.0892	23	24
atmPrf_C2E3.2022.016.01.45.R04_0001.0001_nc	165.9369	-22.7931	1	41
atmPrf_C2E4.2022.016.02.47.G02_0001.0001_nc	162.7582	-17.231	2	45
atmPrf_C2E4.2022.016.02.58.G16_0001.0001_nc	165.553	-19.6844	2	58
atmPrf_C2E2.2022.016.03.10.G02_0001.0001_nc	167.2092	-17.463	3	7
atmPrf_C2E2.2022.016.03.23.G26_0001.0001_nc	176.6833	-18.2854	3	23
atmPrf_C2E5.2022.016.03.54.G16_0001.0001_nc	168.662	-17.5328	3	54
atmPrf_C2E5.2022.016.05.27.G15_0001.0001_nc	165.2896	-17.7996	5	24
atmPrf_C2E2.2022.016.06.34.G12_0001.0001_nc	171.0468	-19.1492	6	31

To verify our BA peak estimated from COSMIC-2 RO data, we further checked the CALIPSO overpass on 16 January 2022. We find an overpass between ~2:59 - 3:12 UTC over the volcanic cloud region (Fig. 4b). Interestingly, there was a collocated COSMIC-2 RO profile with the volcanic cloud at the same time. The obtained BA anomaly was plotted and shown in Figure 4c, respectively. We find close agreement between the RO estimated peak change in the BA height and CALIPSO aerosol plume height. CALIOP observations of aerosol subtypes (Fig. 4b) confirmed the presence of sulfate aerosols near ~29km, strongly supporting the volcanic cloud height reaching the upper stratosphere. The COSMIC-2 RO estimated the height of the BA peak change at 3:07 UTC to be ~29 km which very well matches the presence of a stratospheric aerosol layer at ~29 km. This further provided evidence that the estimated peak of BA height at 5:17 UTC was correct and confirmed that the Tonga volcanic plume rose above the altitudes of ~36 km, respectively.

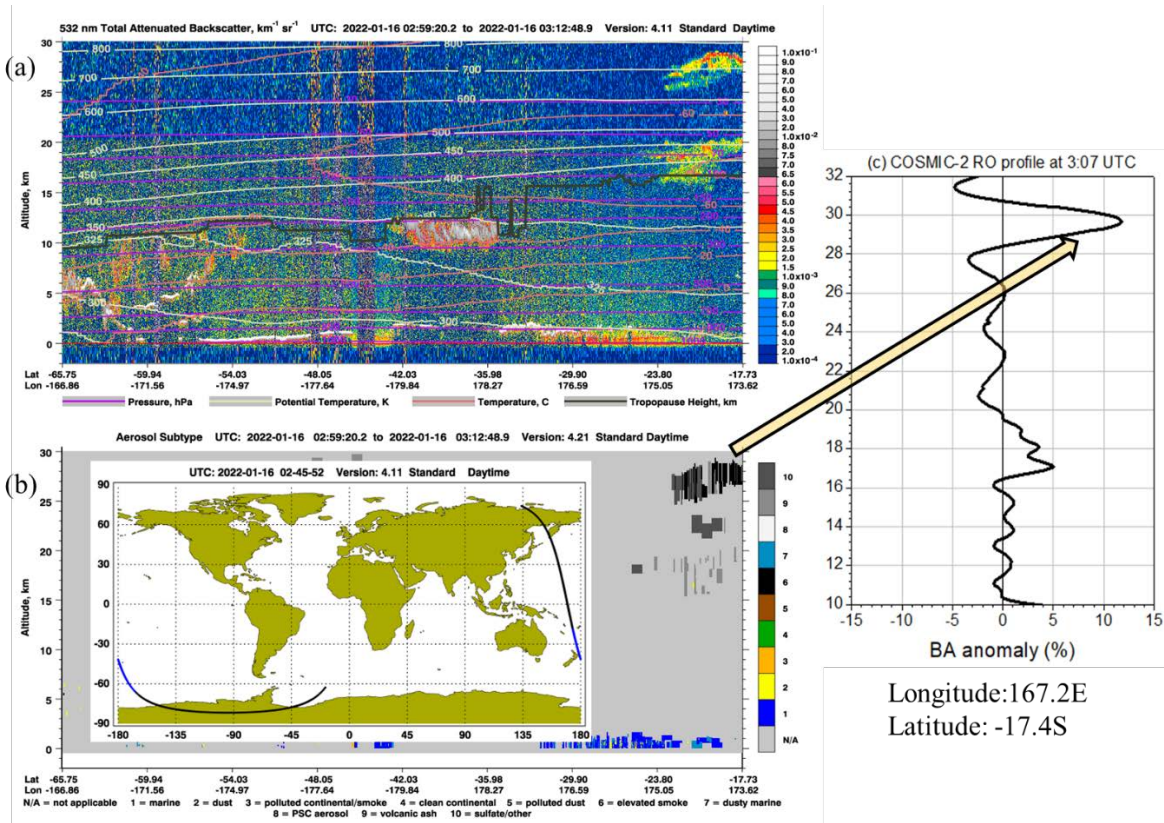


Figure 4. (a) CALIPSO 532 nm total attenuated backscatter coefficient and (b) the CALIPSO aerosol subtypes at @3 UTC on 16 January 2022. The available COSMIC-2 RO bending angle anomaly at 3:07 UTC on 16 January 2022 was also over-plotted within subplot b, respectively.

The observed extreme height of the Tonga volcanic plume can be explained partially by the instantaneous warming due to the pronounced enhancement of the WV. As Tonga volcano was a submarine volcano and erupted highly explosive, it was expected that it emitted tremendous amounts of WV into the stratosphere and the volcanic ash and SO₂. The MLS measurements of WV observed on 16 January 2022, shortly after the initial eruption further support this (**Fig. 5**). Unfortunately, on 15 January we don't have an MLS satellite overpass over the Tonga volcano during its active eruption. However, we noticed extremely high values of stratospheric WV on 16 January in both day and night time overpass periods. **Figure 5** shows that the stratospheric WV mixing ratios exceeded much more than 30 ppm shortly after the eruption downwind of the injection location. Even, the enhancement in the WV was observed at 10 hPa indicating that volcanic WV was directly injected into the upper stratospheric regions. This direct injection of WV might be due to the extreme explosion of the Tonga eruption via the phreatomagmatic interaction of magma and seawater.

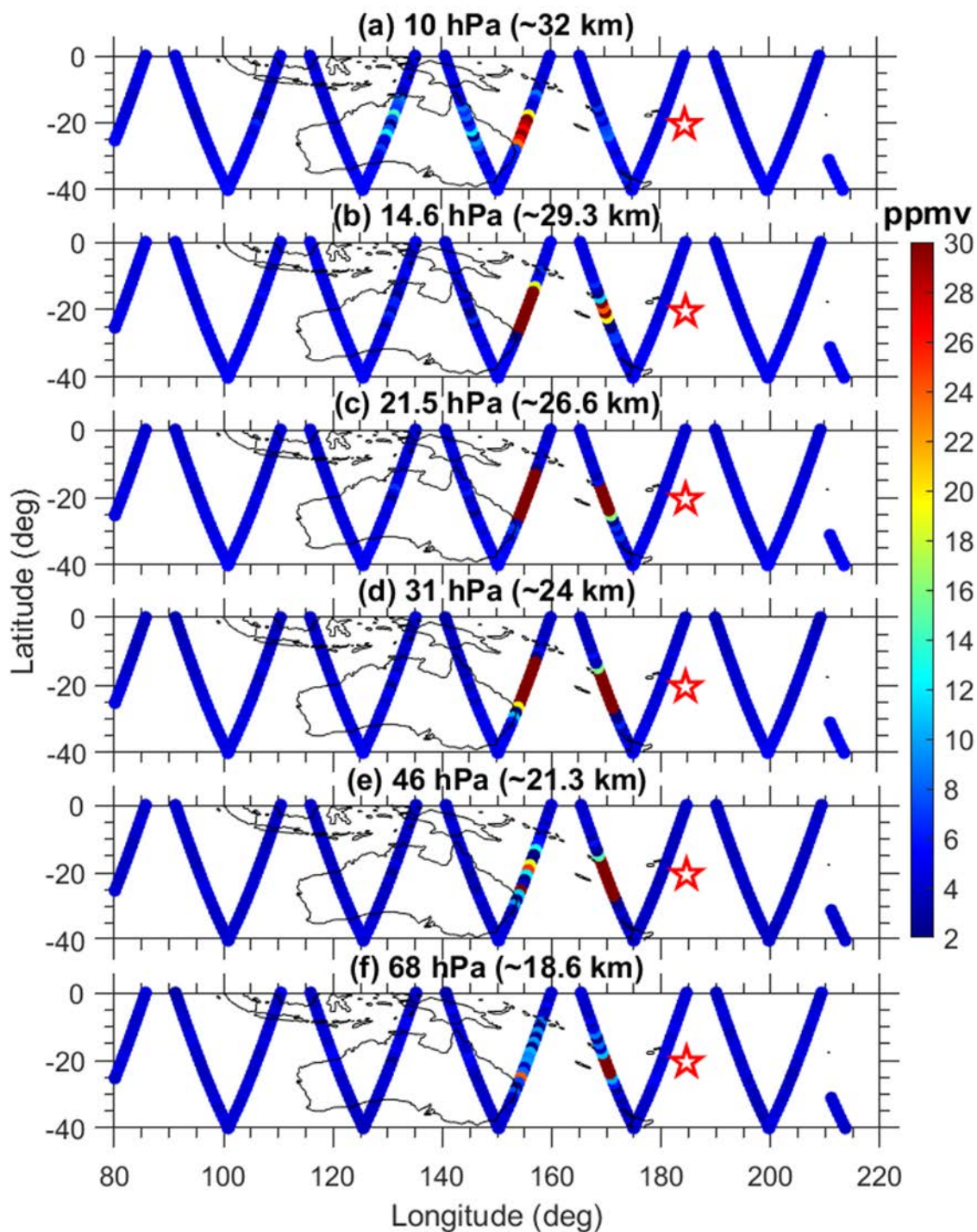


Figure 5. Map of water vapor mixing ratio at different levels from the Microwave Limb Sounder (MLS) measurements observed at two local times, 12 h apart, on 16, January 2022. Middle afternoon sampling runs southeast to northwest, while nighttime observations run northeast to southwest. The red-colored rectangle represents the location of the Tonga volcano.

Few studies reported satellite evidence for the direct injection of WV during the volcanic eruption (Sirois et al., 2016a, b). Even a few studies also reported the injection of volcanic WV for the Pinatubo eruption (Joshi and Jones, 2009; Nedoluha et al., 1998). Recent studies also highlighted the impact of the Tonga eruption on the unprecedented increase of stratospheric WV. Tonga eruption on 15 January injected extreme WV into the stratosphere than previously seen in the modern satellite record (Mill'an et al., 2022). MLS measurements recorded (far exceeding any previous values in the 17-year MLS record)

exceptionally high WV values in the stratosphere after the Tonga eruption indicate (Mill' an et al., 2022). A recent preliminary study by Wright et al. (2022) also highlighted the role of latent heat within the Tonga plume in generating the gravity waves during the 15 January Tonga eruption. They concluded that the latent heat release from the plume remained the most significant individual gravity wave source worldwide for >12 hours, producing circular wavefronts visible across the Pacific basin in satellite observations.

As the Tonga volcanic vent was only tens to hundreds of meters below water, the seawater did not suppress the blast, but was flash-boiled and propelled into the stratosphere (Witze et al., 2022) and rapidly launched a plume of super-heated ash and WV upwards into the atmosphere. Here is condensed, releasing latent heat near-instantaneously across a depth of tens of kilometers. This strong and short-lived force would produce instantaneous warming in the volcanic plume. The instantaneous latent heat release will continue to add to the positive buoyancy of the volcanic plume, allowing it to reach even greater heights as observed during the Tonga eruption. Overall, it is concluded that the thermal energy emitted by the Tonga eruption and the instantaneous release of latent heat induced by the condensation of WV within the eruptive plume, are potential sources of unusual temperature structure and extreme height of the umbrella cloud of Tonga eruption on 15 January.

3.2. Evolution of bending angle perturbations

Further, we examined the BA perturbations for the collocated RO profiles with the volcanic cloud shortly after the initial eruption. There is a total of 16 RO profiles collocated with the volcanic cloud between 5 UTC on 15 January and 7 UTC on 16 January (approximately 24 hours). The collocated available RO profiles and the OMI-observed upper tropospheric and stratospheric SO₂ column during 15-16 January 2022 are shown in **Figure 6a**. The black dots are the available RO profiles on 15 January and the black star dots for the available RO profiles on 16 January, respectively. The details of available RO profiles shown in **Figure 6a** are presented in **Table 1**. To see the evolution in the BA after the eruption, we generated the reference profile for each RO profile shown in **Figure 6a**. We considered all the available RO profiles during 07-13 January 2022 (one week before the eruption) within the 5° latitude and longitude region around each RO profile. Then we removed the reference profile from each RO profile and estimated the change in the BA as well as temperature. The obtained perturbations of each profile were arranged concerning the time to show the evolution. The evolution of the percentage changes in the BA perturbation after the eruption is detailed in **Figure 6b**. The estimated BA peak altitudes are also overplotted in the respective plots. From collocated RO profiles with the eruptive cloud, we find a clear descending of the peak altitude of the BA change from ~36 km to ~30 km within 24 hours after the initial eruption (**Fig. 6b**).

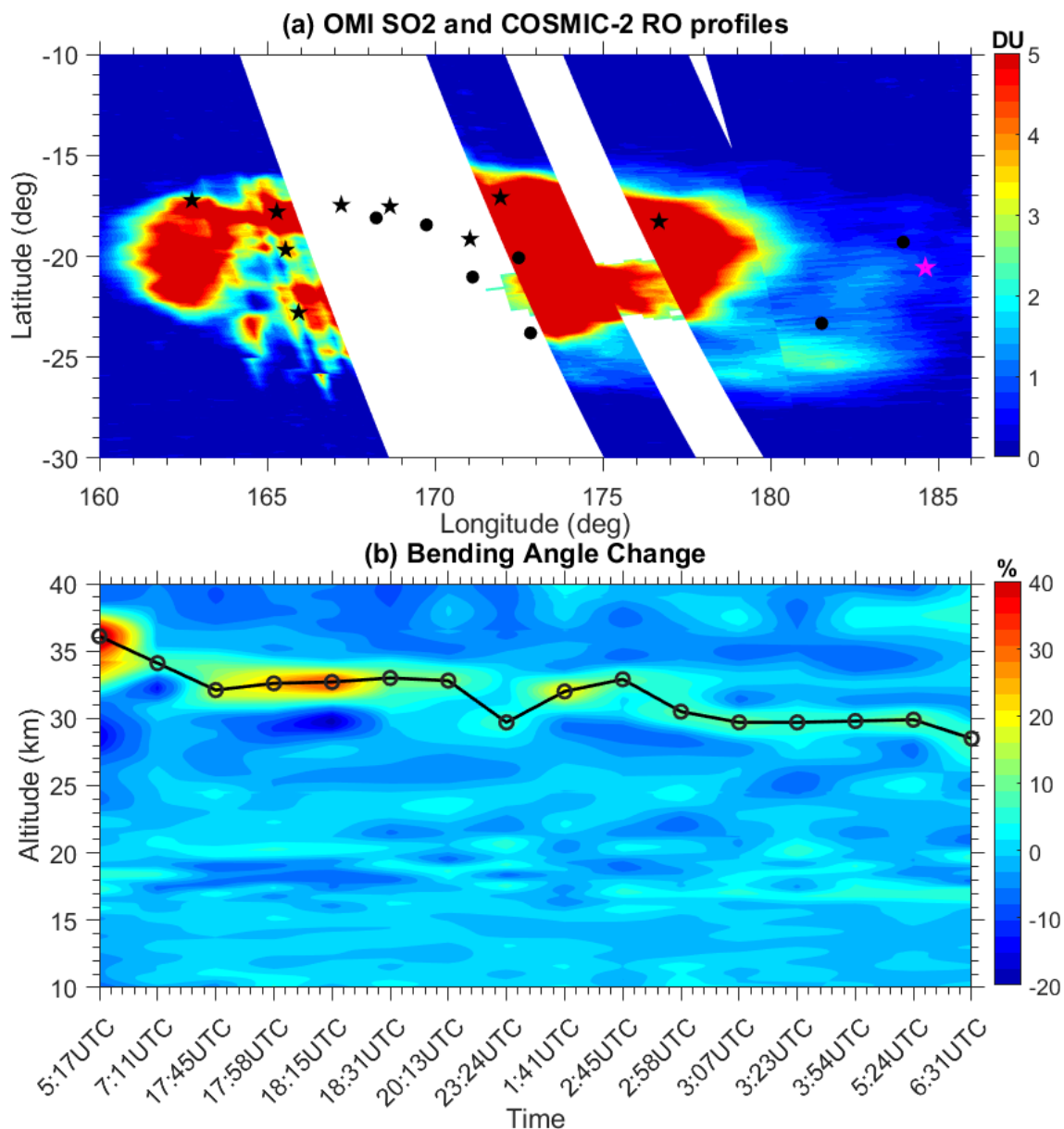


Figure 6. (a) OMI observed UTLS SO₂ on 15-16 January 2022 along with the available COSMIC-2 RO profiles (black dots) on 15-16 January 2022, a time series of the distribution of (b) bending angle (BA) percentage change and the maximum BA peak altitude (black circles), for the above mentioned RO profiles.

4. Summary and Conclusions

The recent eruption of Hunga-Tonga-Hunga-Ha'apai on 15 January 2022 was the largest explosive volcanic event in the satellite era and got immense attention from the scientific community around the world. The explosive blast sent a plume of volcanic ash well into the stratosphere, and even some portion of the plume reached lower mesospheric altitudes. Even though the Mt. Pinatubo eruption was the largest volcanic eruption since 1991, the information about the initial stage of the eruption remains limited (Thomason, 1992). It is reported that the Stratospheric Aerosol and Gas Experiment (SAGE) missed the initial vertical evolution of the volcanic cloud and its injection height (Thomason, 1992). The unprecedented explosive Tonga eruption provided this rare opportunity to describe the volcanic cloud structure, particularly in the stratosphere during the active eruptive phase. By taking this opportunity, the extreme heights and evolution

of the volcanic cloud altitude are reported by using radio occultation measurements from the COSMIC-2 mission.

The schematic diagram explains the plausible mechanisms for the extreme heights of the Tonga eruption on 15 January (**Figure. 7**). As shown in **Figure 5**, the Tonga eruption emitted tremendous amounts of water vapor into the stratosphere along with volcanic ash and sulfur dioxide. MLS satellite measurements from the present study clearly show a tremendous increase in water vapor in the stratosphere after the initial eruption. Recent studies also revealed the large enhancement of stratosphere water vapor due to the Tonga eruption. In the presence of volcanic ash, the WV condensed inside the plume and released latent heat into the plume column. This latent heating can provide additional thermal energy to the plume. The continuing release of the latent heat during the Tonga eruption further added positive buoyancy to the plume, allowing it to reach even greater heights. It is reported earlier that the release of latent heat adds 13% to the thermal energy released by the volcano, which leads to a further plume rise of 1.5 km (Herzog et al. 1998). Our results are also supported by the recent study by Wright et al. (2022). They reported that the latent heat within the plume is the most significant source of generating the gravity waves during the Tonga eruption. It is observed that the large enhancement of stratospheric WV from the MLS measurements along with the volcanic material during the Tonga eruption, clearly confirms that an instantaneous release of heat due to the condensation of water vapor might be one of the additional plausible driving forces along with the explosive volcanic heat to loft the Tonga volcanic plume to higher heights on 15 January. Overall, based on the present results, it is concluded that the thermal energy emitted by the Tonga eruption and the instantaneous release of latent heat induced by the condensation of WV within the eruptive plume, are potential sources of higher volcanic cloud heights. The observed results from the present study provide some more insights into a better understanding of the volcanic plume dynamics. Further, results suggest that all-weather capability, high accuracy, and high vertical resolution measurements from COSMIC-2 RO play an important role in advancing our understanding of the volcanic cloud structure and its implementation in plume modeling. The results from the MLS satellite also highlighted the tremendous amount of WV added to the stratosphere shortly after the initial eruption. This WV may affect a variety of stratospheric chemistry processes, particularly ozone depletion. The detailed evolution and transport of the Tonga plume and its impact on the stratospheric WV changes and the thermal structure variability can be done in future studies.

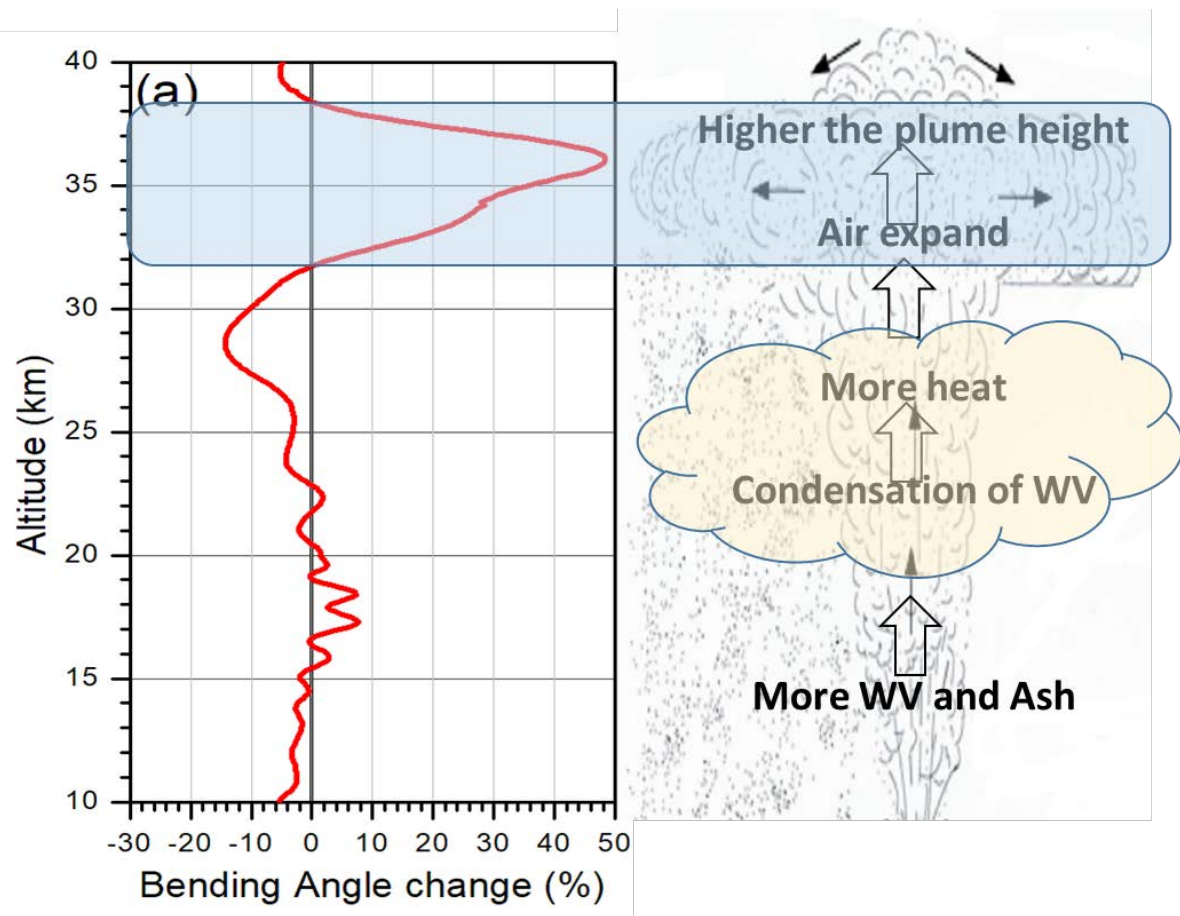


Figure 7. Schematic diagram summarizing the observed extreme heights of Tonga volcanic plume on 15 January. .

Competing Interest : The authors declare that they have no conflict of interest.

Acknowledgments: Ministry of Science and Technology, Taiwan primarily supports the work, under the grants of MOST 110-2811-M-008-562 and MOST 109-2811-M-008-553. The authors thank the COSMIC Data Analysis and Archive Centre (CDAAC) for providing COSMIC-2 data used in the present study through its FTP site (<https://data.cosmic.ucar.edu/gnss-ro/cosmic2/nrt/level2/>). Aura MLS observations were obtained from the GES DISC through their FTP site (https://ac-disc.gesdisc.eosdis.nasa.gov/data/Aura_MLS_Level2/ML2H2O.005). We also thank NASA for providing the Aura Ozone Monitoring Instrument (OMI) data (https://aura.gesdisc.eosdis.nasa.gov/data/Aura_OMI_Level2/OMSO2.003/2020) and the CALIPSO standard images (<https://www-calipso.larc.nasa.gov/>).

References

- Adam, D.: Tonga volcano eruption created puzzling ripples in earth's atmosphere. *Nature*, doi: 10.1038/d41586-022-00127-1. <https://www.nature.com/articles/d41586-022-00127-1>, 2022.
- Anselmo, T.: Cloud-aerosol LIDAR infrared pathfinder satellite observations: Data management system, data products catalog. Document No: PC-SCI-503, NASA, Langley Research Center, Hampton, VA, USA, 2006.
- Anthes, R. A., Bernhardt, P. A., Chen, Y., Cucurull, L., Dymond, K. F., Ector, D., Healy, S. B., Ho, S.-H., Hunt, D. C., Kuo, Y.-H., Liu, H., Manning, K., McCormick, C., Meehan, T. K., Randel, W. J., Rocken, C., Schreiner, W. S., Sokolovskiy, S. V., Syndergaard, S., Thompson, D. C., Trenberth, K. E., Wee, T.-K., Yen, N. L., and Zeng, Z.: The COSMIC/Formosat 3 mission: Early results, *B. Am. Meteorol. Soc.*, 89, 313–333, 2008.
- Astafyeva, E., Maletskii, B., Mikesell, T. D., Munaibari, E., Ravanelli, M., Coisson, P., et al.: The 15 January 2022 Hunga Tonga eruption history as inferred from ionospheric observations. *Geophysical Research Letters*, 49, e2022GL098827. <https://doi.org/10.1029/2022GL098827>, 2022.

- Biondi, R., Steiner, A. K., Kirchengast, G., Brenot, H., and Rieckh, T.: Supporting the detection and monitoring of volcanic clouds: A promising new application of Global Navigation Satellite System radio occultation, *Adv. Sp. Res.* 60, 2707–2722. <https://doi.org/10.1016/j.asr.2017.06.039>, 2017.
- Carvajal, M., Sepulveda, I., Gubler, A., & Garreaud, R.: Worldwide signature of the 2022 Tonga volcanic tsunami. *Geophysical Research Letters*, 49. <https://doi.org/10.1029/2022GL098153>, 2022.
- Carr, J. L., Horváth, Á., Wu, D. L., & Friberg, M. D.: Stereo Plume Height and Motion Retrievals for the Record-Setting Hunga Tonga-Hunga Ha’apai Eruption of 15 January 2022. *Geophysical Research Letters*, 49, e2022GL098131. <https://doi.org/10.1029/2022GL098131>, 2022.
- Coffey, M. T.: Observations of the impact of volcanic activity on stratospheric chemistry, *J. Geophys. Res.-Atmos.*, 101, 6767–6780. <https://doi.org/10.1029/95JD03763>, 1996.
- Global Volcanism Program.: Report on hunga tonga-hunga ha’apai (tonga). *Bulletin of the Global Volcanism Network*, Smithsonian Institution, 40:1. doi: <https://doi.org/10.5479/si.GVP.BGVN201501-243040>, 2022.
- Graf, H.-F., Herzog, M., Oberhuber, J. M., and Textor, C.: The effect of environmental conditions on volcanic plume rise, *J. Geophys. Res.*, 104, 24 309–24 320, 1999. <https://doi.org/10.1029/1999JD900498>, 1999.
- Glaze, L.S., Baloga, S.M., Wilson, L.: Transport of atmospheric water vapor by volcanic eruption columns, *J. Geophys. Res.* 102, 6099–6108, <https://doi.org/10.1029/96JD03125>, 1997.
- Herzog, M., Graf, H.-F., Oberhuber, J.M., Textor, C.: The effect of phase changes of water on the development of volcanic plumes, *J. Volcanol. Geotherm. Res.* 87, 55–74, [https://doi.org/10.1016/S0377-0273\(98\)00100-0](https://doi.org/10.1016/S0377-0273(98)00100-0), 1998.
- Ho, S.-P., Anthes, R.A., Ao, C.O., Healy, S., Horanyi, A., Hunt, D., Mannucci, A.J., Pedatella, N., Randel, W., Simmons, A., Steiner, A.K., Xie, F., Yue, X., Zeng, Z.: The COSMIC/ FORMOSAT-3 radio occultation mission after 12 years: accomplishments, remaining challenges, and potential impacts of COSMIC-2, *B. Am. Meteorol. Soc.* 101, E1107–E1136. <https://doi.org/10.1175/BAMS-D-18-0290.1>, 2019.
- Joshi, M. M. and Jones, G. S.: The climatic effects of the direct injection of water vapour into the stratosphere by large volcanic eruptions, *Atmospheric Chemistry and Physics*, 9, 6109–6118, <https://doi.org/10.5194/acp-9-6109-2009>, 2009.
- Li, C., Krotkov, N. A., Carn, S., Zhang, Y., Spurr, R. J. D., Joiner, J.: New-generation NASA Aura Ozone Monitoring Instrument (OMI) volcanic SO₂ dataset: algorithm description, initial results, and continuation with the Suomi-NPP Ozone Mapping and Profiler Suite (OMPS), *Atmos. Meas. Tech.* 10, 445–458. <https://doi.org/10.5194/amt-10-445-2017>, 2017.
- Livesey, N. J., Read, W. G., Froidevaux, L., Lambert, A., Santee, M. L., Schwartz, M. J., Millán, L. F., Jarnot, R. F., Wagner, P. A., Hurst, D. F., Walker, K. A., Sheese, P. E., and Nedoluha, G. E.: Investigation and amelioration of long-term instrumental drifts in water vapor and nitrous oxide measurements from the Aura Microwave Limb Sounder (MLS) and their implications for studies of variability and trends, *Atmos. Chem. Phys.*, 21, 15409–15430, <https://doi.org/10.5194/acp-21-15409-2021>, 2021.
- Liu, X., Xu, J., Yue, J., & Kogure, M.: Strong gravity waves associated with Tonga volcano eruption revealed by SABER observations. *Geophysical Research Letters*, 49, e2022GL098339. <https://doi.org/10.1029/2022GL098339>, 2022.
- Kubota, T., Saito, T., & Nishida, K.: Global fast-traveling tsunamis driven by atmospheric Lamb waves on the 2022 Tonga eruption. *Science*, 1-8. <https://doi.org/10.1126/science.abo4364>, 2022.
- Kuo, Y.-H., Wee, T.-K., Sokolovskiy, S., Rocken, W., Schreiner, W., Hunt, H., and Anthes, R. A.: Inversion and Error Estimation of GPS Radio Occultation Data, *J. Meteorol. Soc. Jpn.*, 82, 507–531, 2004.
- Kursinski, E. R., Hajj, G. A., Schofield, J. T., Linfield, R. P., and Hardy, K. R.: Observing Earth’s atmosphere with radio occultation measurements using the Global Positioning System, *J. Geophys. Res.* 102, 23429–23465. <https://doi.org/10.1029/97JD01569>, 1997.
- Matoza, R. S., Fee, D., Assink, J. D., Iezzi, A. M., Green, D. N., Kim K., et al.: Atmospheric waves and global seismoacoustic observations of the January 2022 Hunga eruption. *Tonga. Science*, 1-11. <https://doi.org/10.1126/science.abo7063>, 2022.
- NASA Earth Observatory (19 January, 2022): Hunga Tonga-Hunga Ha’apai Erupts. <https://earthobservatory.nasa.gov/images/149347/hunga-tonga-hunga-haapai-erupts>, 2022.
- NASA Earth Observatory (21 January, 2022): Dramatic Changes at Hunga Tonga-Hunga Ha’apai. <https://earthobservatory.nasa.gov/images/149367/dramatic-changes-at-hunga-tonga-hunga-haapai>, 2022.
- NASA Earth Observatory. Tonga Volcano Plume Reached the Mesosphere, 2022.
- Nedoluha, G. E., Bevilacqua, R. M., Gomez, R. M., Siskind, D. E., Hicks, B. C., Russell, J. M., and Connor, B. J.: Increases in middle atmospheric water vapor as observed by the Halogen Occultation Experiment and the ground-based

- Water Vapor Millimeter-Wave Spectrometer from 1991 to 1997, *Journal of Geophysical Research: Atmospheres*, 103, 3531–3543, <https://doi.org/10.1029/97JD03282>, 1998.
- Okazaki, I., and Heki, K.: Atmospheric temperature changes by vol-canic eruptions: GPS radio occultation observations in the 2010 Icelandic and 2011 Chilean cases, *J. Volcanol. Geoth. Res.* 245–246, 123–127. <https://doi.org/10.1016/j.jvolgeores.2012.08.018>, 2012.
- Prata, A.T., Folch, A., Prata, A.J., Biondi, R., Brenot, H., Cimarelli, C., Corradini, S., Lapierre, J., Costa, A.: Anak Krakatau triggers volcanic freezer in the upper troposphere, *Sci. Rep.* 10, 3584. <https://doi.org/10.1038/s41598-020-60465-w>, 2020.
- Proud, S.R, Prata, A., Schmauss, S.: The January 2022 eruption of Hunga Tonga-Hunga Ha’pai volcano reached the mesosphere, *Earth and Space Science Open Archive*, <https://doi.org/10.1002/essoar.10511092.1>, 2022.
- Ramaswamy, V., Chanin, M.-L., Angell, J., Barnett, J., Gaffen, D., Gelman, M., Keckhut, P., Koshel'kov, Y., Labitzke, K., Lin, J.-J. R., O'Neill, A., Nash, J., Randel, W., Rood, R., Shine, K., Shiotani, M., Swinbank, R.: Stratospheric temperature trends: Observations and model simulations. *Reviews of Geophysics*, 39.1, 71–122. <https://doi.org/10.1029/1999RG000065>, 2001.
- Ravindra Babu, S., and Liou, Y. A.: Day-to-day variability of upper troposphere and lower stratosphere temperature in response to Taal volcanic eruption inferred from COSMIC-2 RO measurements, *Journal of Volcanology and Geothermal Research*, Volume 421, 2022, 107445, ISSN 0377-0273, <https://doi.org/10.1016/j.jvolgeores.2021.107445>, 2022.
- Robock, A.: Volcanic eruptions and climate. *Reviews of Geophysics*, 38, 191–219. <https://doi.org/10.1029/1998RG000054>, 2000.
- Schreiner, W., Rocken, C., Sokolovskiy, S., Syndergaard, S., and Hunt, D.: Estimates of the precision of GPS radio occultations from the COSMIC/FORMOSAT-3 mission, *Geophys. Res. Lett.*, 34, L04808, doi:10.1029/2006GL027557, 2007.
- Schreiner, W.S., Weiss, J.P., Anthes, R.A., Braun, J., Chu, V., Fong, J., Zeng, Z.: COSMIC-2 radio occultation constellation: first results, *Geophys. Res. Lett.* 47, 1–7. <https://doi.org/10.1029/2019GL086841>, 2020.
- Self, S., and Walker, G. P. L.: Ash clouds: characteristics of eruption columns, *U.S. Geol. Surv. Bull.* 2047:65–73, 1994.
- Sioris, C. E., Malo, A., McLinden, C. A., and D'Amours, R.: Direct injection of water vapor into the stratosphere by volcanic eruptions, *Geophys. Res. Lett.*, 43, 7694–7700, <https://doi.org/10.1002/2016GL069918>, 2016a.
- Sioris, C. E., Zou, J., McElroy, C. T., Boone, C. D., Sheese, P. E., and Bernath, P. F.: Water vapour variability in the high-latitude upper troposphere – Part 2: Impact of volcanic eruptions, *Atmos. Chem. Phys.*, 16, 2207–2219, <https://doi.org/10.5194/acp-16-2207-2016>, 2016b.
- Taha, G., Loughman, R., Zhu, T., Thomason, L., Kar, J., Rieger, L., & Bourassa, A. (2021). OMPS LP Version 2.0 multi-wavelength aerosol extinction coefficient retrieval algorithm. *Atmospheric Measurement Techniques*, 14(2), 1015–1036. <https://doi.org/10.5194/amt-14-1015-2021>
- Thomason, L. W.: Observations of a new SAGE II aerosol extinction mode following the eruption of Mt. Pinatubo, *Geophysical Research Letters*, 19(21), 2179–2182. <https://doi.org/10.1029/92gl02185>, 1992.
- Tournigand, P.-Y., Cigala, V., Lasota, E., Hammouti, M., Clarisse, L., Brenot, H., Prata, F., Kirchengast, G., Steiner, A. K., and Biondi, R.: A multi-sensor satellite-based archive of the largest SO₂ volcanic eruptions since 2006, *Earth Syst. Sci. Data*, 12, 3139–3159, <https://doi.org/10.5194/essd-12-3139-2020>.
- Wang, K.Y., Lin, S.C., Lee, L.C.: Immediate impact of the Mt Chaiten eruption on atmosphere from FORMOSAT-3/COSMIC constellation, *Geophys. Res. Lett.* 36, L03808. <https://doi.org/10.1029/2008GL036802>, 2009.
- Witze, A.: Why the Tongan eruption will go down in the history of volcanology. *Nature* 316 d41586-022-00394-y (2022) doi:10/gpfhcm, 2022.
- Woods, A.W.: Moist convection and the injection of volcanic ash into the atmosphere. *J. Geophys. Res.* 98, 17627–17636, 1993.
- Woods, A.W.:The dynamics of explosive volcanic eruptions. *Rev. Geophys.* 33, 495–5, <https://doi.org/10.1029/95RG02096>, 1995.
- Woods, A., and Self, S.: Thermal disequilibrium at the top of volcanic clouds and its effect on estimates of the column height, *Nature* 355, 628–630, <https://doi.org/10.1038/355628a0>, 1992.
- Wright, C., Hindley, N., Alexander, M.J., Barlow, M., Hoffmann, L., Mitchell, C., Prata, F., Bouillon, M., Carstens, J., Clerbaux, C., Osprey, S., Powell, N., Randall, C., and Yue, J.: Surface-to-space atmospheric waves from Hunga Tonga-Hunga Ha’apai eruption, *Earth and Space Science Open Archive*, <https://doi.org/10.1002/essoar.10510674.2>, 2022.

Young, S. A., Vaughan, M. A.: The retrieval of profiles of particulate extinction from Cloud Aerosol Lidar Infrared Pathfinder Satellite Observations (CALIPSO) data: Algorithm description. *Journal of Atmospheric and Oceanic Technology.*, **26**, 1105– 1119, <https://doi.org/10.1175/2008JTECHA1221.1>, 2009.

Zuo, M., Zhou, T., Man, W., Chen, X., Liu, J., Liu, F., Gao., C.: Volcanoes and Climate: Sizing up the Impact of the Recent Hunga Tonga-Hunga Ha’apai Volcanic Eruption from a Historical Perspective. *Adv. Atmos. Sci.* <https://doi.org/10.1007/s00376-022-2034-1>, 2022